Evaluation of MOCAGE chemistry transport model during the ICARTT/ITOP experiment

N. Bousserez,[1] J.L. Attié,[1] V.H. Peuch,[2] M. Michou,[2] G. Pfister,[3] D. Edwards,[3] L. Emmons,[3] S. Arnold,[4] A. Heckel[5] A. Richter,[5] H. Shlager,[6] A. Lewis,[7] M. Avery,[8] G. Sachse,[8] E. Browell,[8] and R. Ferrare[8]

N. Bousserez, OMP (Laboratoire d'Aérologie), 14 avenue Edouard Belin, 31400 Toulouse, France. (boun@aero.obs-mip.fr)

[1]Laboratoire d'Aérologie, Université Paul Sabatier, Toulouse, France.

[2]Centre National de Recherches météorologiques/Météo France, Toulouse, France.

[3]National Center for Atmospheric Research (NCAR), Boulder, USA.

[4]Institute for Atmospheric Science, University of Leeds, UK

[5]Institute of Environmental Physics, Bremen, Germany

Abstract.

We evaluate the Météo-France global chemistry transport 3D model MOCAGE (MOdèle de Chimie Atmosphérique à Grande Echelle) using the important set of aircraft measurements collected during the ICARRT/ITOP experiment. This experiment took place between US and Europe during summer 2004 (July 15-August 15). Four aircraft were involved in this experiment providing a wealth of chemical data in a large area including the North East of US and western Europe. The model outputs are compared to the following species of which concentration is measured by the aircraft: OH, H_2O_2, CO, NO, NO_2, PAN, HNO_3, isoprene, ethane, HCHO and O_3. Moreover, to complete this evaluation at larger scale, we used also satellite data such as SCIAMACHY NO_2 and MOPITT CO. Interestingly, the comprehensive dataset allowed us to evaluate separately the model representation of emissions, transport and chemical processes. Using a daily emission source of biomass burning, we obtain a very good agreement for CO while the evaluation of NO_2 points out incertainties resulting from inaccurate ratio of emission factors of NO_x/CO. Moreover, the chemical behavior of O_3 is satisfactory as discussed in the paper.

1. Introduction

Modeling constitutes an essential complement to filling gaps in temporal and spatial coverage of *in situ* and remote sensing measurements. Numerous studies have shown the capacity of global chemistry transport models (CTM) to reproduce the main characteristics of the atmospheric chemical composition [*Bey et al.*, 2001; *Wang et al.*, 1998; *Horowitz et al.*, 2003]. These successes have led to the use of CTM for chemical forecast [*Dufour et al.*, 2005], satellite retrievals [*Palmer et al.*, 2001] and climate predictions [*Dentener et al.*, 2006]

The MOCAGE (MOdèle de Chimie Atmosphérique à Grande Echelle) model is a 3-D CTM which has been developped at the Centre National de Recherches Météorologiques (Météo-France). Among current CTMs, MOCAGE presents several specificities. First, it is a multi-scale model, covering scales from regional with a high resolution down to 0.1°x 0.1°to planetary with the resolution of 2°x 2°allowing the representation of small scale dynamic processes. Moreover, it combines tropospheric and stratospheric chemistry, which is important in e.g. ozone budget studies [*Rivière et al.*, 2005]. Finally, it uses a very detailed tropospheric chemical scheme RACM (Regional Atmospheric Chemistry Mechanim) [*Stockwell et al.*, 1997]. This makes MOCAGE a very attractive model allowing it to cover a wide range of scientific objectives, from the chemical data assimilation [*Pradier et al.*, 2006] to the modeling of tropospheric chemistry at a regional scale [*Dufour et al.*, 2003].

During summer 2004, the European Intercontinental Transport of Ozone and Precursors (ITOP) was conducted as part of ICARTT [*Fehsenfeld*, 2006]. Several scientific teams from Germany, France, the UK and the US carried out aircraft measurements of chemical species concentrations between N. America and Europe were involved in this experiment. The aim of this project was to better understand the mechanisms of pollution chemistry within up-lifted air exported from N. America to Europe. The campaign took place between July 15 and August 15, 2004. Strong wildfires over North America and Canada occurred with a high variability both in space and time and created rich pollution air plumes reaching the coasts of Europe and releasing numerous species in the atmosphere. The summer of 2004 was one of the strongest fire seasons on record for Alaska and Western Canada. The number of species simultaneously measured, the frequency of sampling, together with the large area considered, make this campaign a very useful data base for the evaluation of models.

During this campaign, MOCAGE was used to provide chemical forecast and analysis to help defining the experimental aircraft flight plans.

We present in section 2 the model set-up and the data used for this model evaluation (section 3). The results from the MOCAGE (Version 1.0) simulation in the period of the ITOP experiment are presented in section 4. In that section we compare modeled and observed concentrations of ozone and related trace gases using aircraft *in-situ* measurements and satellite data from the intruments MOPITT (Measurement Of Pollution In The Troposphere)[*Drummond and Mand*, 1996] and SCIAMACHY (SCanning Imaging

Absorption spectroMeter for Atmospheric CHartographY)[*Bovensmann, H. et al.*, 1999]. Finally, we conclude in section 5.

2. Model set-up

The MOCAGE model is a global 3-D CTM providing numerical simulations of the interactions between dynamical, physical and chemical processes in the troposphere and lower stratosphere. MOCAGE uses a semi-lagrangian gridpoint model [*Josse et al.*, 2004] to transport the species. For our simulation we used the global grid with a horizontal resolution of 2°x 2°. MOCAGE includes 47 hybrid (σ, P) levels from the surface up to 5 hPa. The vertical resolution is 40 to 400 m in the boundary layer (7 levels) and about 800 m in the lower stratosphere and in the vicinity of the tropopause. The chemical scheme used is RACMOBUS, which combines the stratospheric scheme REPROBUS [*Lefèvre et al.*, 1994] and the tropospheric scheme RACM [*Stockwell et al.*, 1997]. RACMOBUS includes 119 individual species, among which 89 are prognostic variables, and considers 372 chemical reactions. Convective processes are simulated with the scheme of *Bechtold et al.* [2001], and turbulent diffusion is calculated with the scheme of *Louis* [1979]. MOCAGE also parameterizes emissions and dry deposition [*Michou and Peuch*, 2002; *Michou et al.*, 2005; *Nho-Kim et al.*, 2004], and scavenging. MOCAGE uses the emission inventory from *Dentener et al.* [2004, 2006] with a monthly or yearly resolution depending on the species. However, because of numerous wildfire events that occurred over N. America during the ICARTT/ITOP campaign, we modified the emissions of several species using the daily US emission inventory of *Pfister et al.* [2005]. The source emissions are just injected from the surface. For more details concerning the sources inventories used in the model see Table 1. The meteorological analyses of Météo-France ARPEGE [*Courtier et al.*, 1991]

were used to initialize and constrain the dynamics of the model every 6 hours. The vertical velocity is calculated from the ARPEGE wind horizontal components by imposing the mass conservation law for each atmospheric column.

Figure 1 shows the MOPITT CO concentrations binned at 0.5°x 0.5°at 500 hPa during the ITOP period (2004/07/15 to 2004/08/15), along with the corresponding horizontal wind field obtained from ARPEGE meteorological analyses. We see typical summertime features of the atmospheric circulation with a strong high above the western Atlantic and a low near the British Islands. Because of its long residence time, CO is known as a good tracer of polluted air masses and clearly shows here the pathway of exported pollution over the Atlantic, centered at about 50°N. Maximum CO concentrations are localized over Alaska and Canada due to the wildfire events during this period. The strong zonal flow above Alaska and the following deep thalweg allow a rapid transport of pollutants to the N. E. US. The polluted plumes subsequently undergo a strong South West outflow. Our simulation started from a climatological initial field on June 1, 2004 at 12 UT.

3. Rationale of the evaluation

3.1. Chemical species

We focused our evaluation of MOCAGE on the following species: OH, H_2O_2, CO, NO, NO_2, PAN, HNO_3, Isoprene, Ethane, formaldehyde (HCHO) and O_3. OH is the main oxidant for non-radical species in the atmosphere. Its concentration is of primary importance for quantifying chemical processes in the troposphere, in particular the formation and destruction of O_3. The radical OH is formed by O_3 photolysis as follow:

$$O_3 + h\nu \rightarrow O_2 + O(^1D)$$

$$O(^1D) + H_2O \rightarrow 2OH$$

Besides its fundamental role in tropospheric chemistry as principal OH source, the O_3 molecule is known as being toxic to humans and vegetation because it oxidizes biological tissue. In the troposphere, O_3 can be produced by oxidation reactions between OH and some trace gas constituents. Moreover, H_2O_2 is a reservoir for HO_x ($HO_x = H+OH+HO_2$) in the atmosphere.

CO produced by incomplete combustion of hydrocarbons, plays a key role in tropospheric chemistry as ozone precursor. The chain mechanism [*Jacob*, 2000] leading to O_3 production consists in the oxidation of CO by O_2 which is catalyzed by the HO_x family and by $NO_x = NO + NO_2$. The lifetime of CO at mid-latitudes is about one month. Oxidation of hydrocarbons follows the same scheme as CO oxidation and is of primary importance in the regulation of tropospheric OH and O_3 concentrations. Ethane is released by industrial and combustion sources and is removed by OH oxidation with a lifetime of a few months. HCHO is a by-product of hydrocarbons oxidation. It can be scavenged by clouds but its lifetime is long enough to allow transport in remote region where its photolysis produces HO_x radicals. The principal biogenic hydrocarbon contributing to O_3 formation is isoprene, an odorless compound which is a by-product of photosynthesis. Isoprene reacts extremely rapidly with OH, resulting in an atmospheric lifetime of less than one hour. NO_x is produced by combustion processes, lightning and soil decomposition. NO_x concentrations control to a large part the chemical equilibriums involving O_3

production or destruction in the troposphere and thus play a key role in air quality. The principal sink of NO_x is oxidation by HNO_3. Because of its high solubility in water, HNO_3 is scavenged by precipitation in the troposphere.

PAN is produced in the troposphere by photochemical oxidation of carbonyl compounds in the presence of NO_x. In turn, PAN can regenerate NO_x by thermal decomposition. The lifetime of PAN strongly depends on temperature, varying from 1 hour at 295 K to several months at 250 K. In the lower troposphere, NO_x and PAN are near chemical equilibrium. However, in the middle and upper troposphere PAN is a reservoir for NO_x. It can be transported over long distances and decomposed to release NO_x far from its source.

The ICARTT/ITOP campaign provided *in situ* measurements of all these species. In addition, satellite data allow global observations of pollution.

3.2. The data

The measurements were made aboard several aircraft: FAAM BAE 146 from the Institute for Atmospheric Science (UK), DC-8 from the NASA Project Office (USA), P3 from the NOAA Aeronomy Laboratory (USA), and Falcon from the Institute of Atmospheric Physics (Germany) (see Table 2). MOZAIC (Measurement of OZone and water vapour by AIrbus in-service airCraft) data [*Thouret et al.*, 1998; *Nédélec et al.*, 2003] during the ITOP period are also used. We averaged the datasets over 1-min intervals and performed an on-line comparison to compare modeled and aircraft measurements. The observed and simulated concentrations obtained by this method were subsequently averaged over three regions (Fig.2) : N. E. America, Europe and Atlantic ocean, referred to hereafter as domains 1, 2 and 3, respectively. The number of domains used depend also on the

availability of the aircraft data over the area. In order to evaluate our simulation at a larger scale, we also incorporated MOPITT CO retrievals and NO_2 tropospheric columns from SCIAMACHY.

MOPITT is a nadir Infra-Red correlation radiometer onboard the NASA Terra Satellite. It has a horizontal resolution of 22 kmx22 km and provides a global coverage in about 3 days. We used the Level 2 V3 MOPITT datasets, which consist of retrieved CO mixing ratios for 7 vertical levels in the atmosphere (surface, 850 hPa, 700 hPa, 500 hPa, 350 hPa, 250 hPa and 150 hPa). A detailed description of the MOPITT-CO retrievals, based on radiance inversion, is given in [*Deeter et al.*, 2003]. The number of degrees of freedom in one profile, which characterizes the information content of the retrieval, is typically less than 2 [*Deeter et al.*, 2004]. For the comparisons with the model results, we applied the MOPITT averaging kernels to make comparable the different data.

SCIAMACHY observes the upwelling radiation from the earth surface and the extraterrestrial solar radiance. It alternately measures in nadir and limb, covering the 220-2240 nm spectral region range with a resolution of 0.25 nm in the UV, 0.4 nm in the visible and less than 0.4 nm in the NIR. The typical size of the nadir ground-pixel for NO_2 is 30 km x 60 km. Its swath width is 960 km, providing a global coverage at the equator within 6 days. Here we used the NO_2 tropospheric column product. The retrieval approach used for NO_2 nadir measurements is based on the Differential Optical Absorption Spectroscopy (DOAS) method. Details on the data analysis can be found in *Richter et al.*, [2005].
Note that an on-line comparison was applied to compare MOPITT CO retrievals with MOCAGE CO simulations. In addition, comparisons of NO_2 columns between SCIA-

MACHY and MOCAGE were carried out using an off-line interpolation. The MOCAGE tropospheric columns of NO_2 are calculated from the surface to the tropopause as determined with a PV = 2.

4. Results and discussions

4.1. Hydroxyl Radical and Hydrogen Peroxide

Figures 3 and 4 present the vertical profiles of OH and H_2O_2 respectively. Over domain 1 the model slightly overestimates OH concentrations by 0.1-0.2 pptv in the lower-troposphere. OH concentrations are very sensitive to anthropogenic emissions close to the surface. The model divergence is thus probably linked to inaccuracies in our emission inventory. The good agreement with observations at mid-troposphere attests that the tropospheric chemical equilibrium is well simulated by MOCAGE. Above 8 km, the underestimation of 0.1-0.2 pptv may be due to an underestimation of cloud albedo photochemical effects [*Brune et al.*, 1998] or too low H_2O concentrations. Simulated H_2O_2 concentrations are slightly lower (bias of 500 pptv) than observed concentrations in the low and the middle troposphere of domain 1 but remain within the range of observations. The model reproduces well the decrease of H_2O_2 with increasing altitude due to the airmass drying out. Lower H_2O_2 concentrations from the model between 0 and 5 km are consistent with higher OH concentrations that enhance the reaction: $H_2O_2 + OH \rightarrow HO_2 + H_2O$. Over domain 3, the model overestimates the observed OH concentrations by about 0.36 pptv throughout the troposphere. The bias in lower-troposphere may result from an underestimation of the marine boundary layer cloud cover in ARPEGE [*Mathieu et al.*, 2003] leading to a higher rate of ozone photolysis. More globally, the OH tropospheric bias may be linked to photochemical effects of aerosols not included in MOCAGE [*Duncan et al.*,

1997]: (1) aerosol scattering and absorption of UV radiation, and (2) reactive uptake of HO_2, NO_2 and NO_3. For example, *Martin et al.* [2003] showed that aerosols may decrease boundary layer OH concentrations by a factor 2 over northern Europe during summer and up to a factor 4 over biomass burning regions of North India. During the ITOP period, long range transport (LRT) events were precisely associated with high aerosol concentrations in pollution plumes [*Real et al.*, 2006]. Results for H_2O_2 over domain 3 show an underestimation of about 1000 pptv consistent with the higher oxidizing power of the atmosphere in the model.

4.2. Carbon Monoxide

Figure 5 shows the comparisons between MOCAGE and MOPITT CO at 500 hPa for the period July 15 - August 15, 2004. The model reproduces very well the observed distribution. The main pollution pathway spreads from N.E. America to N.W. Europe, centered around 50°N. The correlation coefficient (r^2) between the model and the observations at this level is approximately 0.98. The histograms (Fig. 5 c) are very comparable though the model tends to slightly overestimate the high and the low values. We calculated the figure of merit defined as the ratio of the surface of the histograms intersection and the surface of the histograms union. Closer to 1 closer the distributions are. The calculated value is 0.66. Figure 6 shows MOPITT and MOCAGE CO at 500 hPa for the period between July 24 and July 26, 2004. This case shows that MOCAGE allows an accurate representation of relative small-scale structures seen by MOPITT, in particular over the Atlantic ocean and N.W. Europe.

Figure 7 displays the aircraft and simulated vertical profiles of CO. Observed profiles are similar over domain 1 and 2 and fairly well reproduced by the model. Maximum values are found in the lower-troposphere due to anthropogenic emissions. Convection processes over continental areas during the summer result in a well mixed middle and upper troposphere. There is a weak CO concentration overestimation of about 10-20 ppbv above 4 km globally remaining within the range of observations. Results for domain 3 show approximately the same bias throughout the troposphere. This bias which is a weak overestimation of modeled CO background is probably due to an overestimation of CO emissions in the model. CO comparisons over domain 3 establish the capability of the model to reproduce accurately the transport processes. Indeed, the two peaks at 6 km and 9 km as well as the high concentration variability linked to LRT events are well reproduced by the model.

4.3. Hydrocarbons and Isoprene

Comparisons of vertical profiles of ethane are shown in Figure 8. For domain 1, there is a good agreement between simulated and observed concentrations above 2 km. The lower troposphere concentrations are underestimated by about 300 pptv but remain within the range of observations. Comparisons for domain 2 show the same behavior as domain 1. However, very few data are available below 8 km altitude.

The global emission inventory for ethane varies in the litterature between 8 and 36 $Tg(C).y^{-1}$. The inventory used in MOCAGE calculates an annual emission rate of 8 $Tg(C).y^{-1}$. However, *Xiao* [2005] found an estimate of 13.5 $Tg(C).y^{-1}$. Thus, the bias between measured and modeled concentrations in the continental Planetary Boundary Layer (PBL) might be due to an underestimation of ethane emissions in the model. In

addition, the higher variability of the observations relative to the simulated values near the ground shows the strong dependence of ethane to emission resolution. For domain 3, the simulated ethane profile is consistent with the observed profile except between 9 and 10 km. The very few data available at those altitudes possibly cause a representativeness error. However, the model reproduces well the two peaks at 3 and 6 km as well as the high variability of the concentrations.

The HCHO comparisons between model results and aircraft observations are presented in Figure 9. Over domain 1, the simulated profile is consistent with the observed profile despite a slight overestimation of about 100 pptv in the middle and upper troposphere. Over domain 3, the shape of the HCHO profile is quite well reproduced by the model. There is a non-systematic weak underestimation outside the PBL probably resulting from too high OH concentrations that shorten the HCHO lifetime by oxidation reactions. Note that oxidation by OH radicals leads to a CO production which can be linked to the CO bias discussed previously. The high variability of observed values compared with the low variability of simulated values reflects these lifetime differences. Indeed, a longer lifetime allows a greater influence of LRT events on concentration profiles. Besides, we note for the observations a nearly constant value with altitude of the order 300 pptv above 5 km, which has been identified in previous studies as the signature of air masses originating from North America [*Helan et al.*, 2003] Figure 10 presents the results of the comparison for isoprene over domain 1. Model concentrations are in quite good agreement with observed concentrations except near the surface where the strong dependence of isoprene emissions to soil nature and vegetation induces a high variability.

4.4. Nitrogen species

Figure 11 compares the NO_2 tropospheric column retrieved by SCIAMACHY and that simulated by MOCAGE for the period between July 15 and August 15, 2004. Globally, the model overestimates NO_2 column concentrations by about 3.10^{14} molec.cm^{-2}. Figure 11c shows that the most pronounced biases are localized over low NO_2 concentration regions i.e. over oceans. However, the shape of histograms from the model and the observations are quite similar with a figure of merit of about 0.67. The NO_2 global field is quite well reproduced by the model except for N.W. America under strong biomass burning.

Turquety et al., [2006] recently estimated that 17 % of the total area burned in Alaska and Canada during the summer 2004 was located in peatlands. In addition, *Bertschi et al.* [2003] studied the emissions from residual smoldering combustion (RSC) and concluded that correcting emission estimates by including RSC could decrease the NO emission factor (EF) by a factor 2. We found that our EF(NO_x)/EF(CO) ratio is more than twice that recommended by *Bertschi et al.* [2003], which could explain the discrepancies observed between SCIAMACHY measurements and MOCAGE simulation over wildfire areas. Finally, the NO_2 concentrations simulated over the Atlantic are very high compared to SCIAMACHY measurements. Note that *Richter and Burrows* [2002] have shown that most of the uncertainties in the derived tropospheric columns using DOAS method result from a contamination by clouds and light path, leading in some cases to an underestimation by up to 40 %. The difference in calculation of tropospheric columns may also explain the bias between MOCAGE and SCIAMACHY NO_2. Moreover, the North Atlantic region is known as being very cloudy during summer [*Mathieu et al.*, 2003] and

this could considerably degrade the accuracy/precision of the retrievals.

A comparison of simulated and observed NO profiles is shown in Figure 12. Over domain 1, the model is in relatively good agreement with the observations for the altitude range 0 to 5 km, while it underestimates the NO concentrations in the upper troposphere by up to 400 pptv. The measured NO profile is typical of lightning activity [*Decaria et al.*, 2005; *Barthe et al.*, 2006]. And indeed, strong lightning activity occurred over domain 1 between July 15 and August 15, 2004 (Fig. 14). Thus the upper troposphere NO bias is likely due to the fact that MOCAGE does not parameterize NO_x production by lightning. Over domain 2 and 3, the simulated NO concentrations are consistent with measurements in the low and mid-troposphere. The slight divergence observed in the upper troposphere is probably also linked to NO production by lightning but is smaller than over domain 1.

Figure 13 shows the simulated and observed NO_2 concentration profiles. Over domain 1, NO_2 concentrations are fairly well reproduced by the model. The weak underestimation in the upper troposphere is less pronounced than for NO because of the very low air density and cold temperatures at this altitude that considerably reduce the speed of the kinetics of the reaction: $NO + O_3 \rightarrow NO_2 + O_2$. Over domain 3, the model underestimates the NO_2 concentrations by about 200 pptv throughout the troposphere. These discrepancies might be explained by the higher OH concentrations in the model resulting in a shorter NO_2 lifetime. Besides, the high variability of the measurements at mid-troposphere compared to the simulated concentrations also seems to indicate a significant influence of LRT events on the measured profiles. Over domain 2, there is a relatively good agreement between

observed and simulated NO_2 concentrations in the lower troposphere except close to the surface where the high variability of measurements makes the comparison difficult. The systematic underestimation of about 200 pptv above 3 km may be due to intercontinental transport, based on the similarity with the bias observed over domain 3.

Concerning PAN concentrations (Fig. 15), the model overestimates observed concentrations by about 500 pptv throughout the troposphere over domain 1. These discrepancies remain within the range of observations in the PBL, where the concentrations are essentially influenced by surface NO_x emissions. Above 2 km, the bias probably results from too high NO_x emission rates over the wildfire areas as pointed out previously, and the subsequent excess of PAN production. Over domain 3, the overestimation is quite similar to that observed over domain 1, except in the lower troposphere where PAN decomposition takes place. The model reproduces both the peak at 6 km and the high variability in mid-troposphere linked to LRT events. Over domain 2, simulated PAN concentrations are consistent with observations at 1 km. However, above 1 km, a systematic bias quite similar to that found over domains 1 and 3 is observed, suggesting the influence of intercontinental transport of pollution. Note that the discrepancies observed near the ground can be due to a representativeness error owing to the very few data available.

For HNO_3 (Fig. 16), simulated concentrations are similar to observed concentrations over domain 1. As expected, the HNO_3 profile is correlated with the NO_2 profile as HNO_3 is produced in the troposphere by oxidation of NO_2. For domain 3, observed concentrations are overestimated by the model in the lower troposphere (from 0 to 3 km) up

to a factor 8 close to the surface. These strong discrepancies have already been mentioned in previous model evaluations [*Horowitz et al.*, 2003] and might be linked to the wet deposition parameterization and inaccurate rain fluxes in the meteorological analyses. In addition, the underestimation of the marine boundary layer cloud cover in ARPEGE analyses may also induce a slower wet deposition near the surface. Moreover, the high OH level simulated in the model and the presence of relatively high NO_2 concentrations could lead to significant production of HNO_3. Above 2 km, observed HNO_3 concentrations are relatively well reproduced by the model except in the upper troposphere where cloud scavenging is probably underestimated.

In order to better understand the chemical processes involved during the transport of polluted air masses, it is useful to consider the NO_y family (NO_y = NO + NO_2 + PAN + HNO_3). Figure 17 shows NO_y profiles comparisons between observations and simulations. Over domain 1, the shape of the profile is relatively well reproduced. The model overestimates observed concentrations by about 500 pptv in the low and mid-troposphere while there is a slight underestimation in the upper troposphere probably due to NO_x production by lightning. Over domain 3, there is approximately the same NO_y overestimation as for domain 1 and we observe a fairly good correlation between the observed and modeled profiles except in the PBL and upper troposphere. Because nitrogen oxides from combustion processes and lightning are mainly emitted as NO_x and converted into NO_y species afterwards, the $[NO_x]/[NO_y]$ ratio can be used as a measure of the age of emissions [*Helan et al.*, 2003].

Figure 18 presents the NO_y partitioning over domain 1 and 3 for both the simulation and the observations. Over domain 1, the global partitioning is quite similar in the model results and the observations. In particular, in the lower troposphere, the contribution of PAN rapidly increases with the altitude while HNO_3 contribution decreases. We also observe that the modeled $[NO_x]/[NO_y]$ ratio decreases with increasing altitude, whereas the observed $[NO_x]/[NO_y]$ ratio increases in the upper troposphere where the lightning NO_x production takes place. Over domain 3, the simulated NO_y distribution is approximately the same as domain 1. Here the weak $[PAN]/[NO_x]$ ratio near the surface is likely due to the thermal decomposition of PAN. The contribution of NO_2 over domain 3 for the observations is higher than model results, which probably reflects differences in air masses reactivity resulting from differences in OH concentrations.

4.5. Ozone

Figure 19 displays O_3 profiles from MOCAGE and from aircraft measurements. The model overestimates O_3 concentrations by about 30 ppbv in the lower troposphere (below 2 km) of domain 1. Several models found a comparable overestimation over the N.E. US, partly resulting from recent changes in isoprene and anthropogenic emissions [*Fiore et al.*, 2005] and from the effect of the horizontal resolution. The bias decreases with increasing altitude and observed and simulated concentrations are in good agreement above 5 km. Over domain 3, the shape of the observed profile is fairly well reproduced despite a mean overestimation of about 18 ppbv throughout the troposphere. *Chandra et al.* [2004] found that over Northern oceans the contribution to the Tropospheric Column Ozone due to stratosphere-troposphere exchange is about 50-55 %. Thus, the relatively good representation of O_3 concentrations in the mid- and upper troposphere might be the sign of

efficient coupling of tropospheric and stratospheric chemistry in MOCAGE. Over domain 2, the shape of the observed profile is quite well reproduced by the model despite a slight overestimation by about 20 ppbv in the lower troposphere.

Several studies have shown relatively robust correlations between O_3 and NO_y [*Helan et al.*, 2003]. We thus calculated ΔO_3 / ΔNO_y ratios, where Δ represents the difference between modeled and observed concentrations. Over domain 1, we found a ΔO_3 / ΔNO_y ratio of about 10 below 2 km and about 33 between 2 and 3 km altitude. These values are in good agreement with those reported in the litterature for this area [*Helan et al.*, 2003]. Over domain 3, we established a ΔO_3 / ΔNO_y ratio of about 50 in the mid-troposphere, which corresponds to the values reported in *Helan et al.* [2001] for marine environment. Simulated O_3 concentrations over domain 2 are relatively consistent with the observations despite a slight overestimation of about 10 ppbv in the mid- and low troposphere. The significant underestimation occurring at 12 km is probably linked to a too elevated tropopause height in the model.

Therefore, our results show that NO_y overestimations explain quite well the bias observed in O_3 concentrations and suggest that the model reproduces relatively well the chemical equilibriums between O_3 and the NO_y family. Note that among the chemical processes leading to an ozone enhancement in pollution plumes during LRT events, the PAN decomposition is identified as a possibly dominant source as pointed out in *Hudman et al.* [2004]. Thus, the slight O_3 overestimation over the Atlantic domain may be linked to the excess of PAN in the model.

5. Conclusion

This paper provides a comprehensive evaluation of the global 3D MOCAGE CTM using aircraft measurements and satellite observations available during the ICARTT/ITOP experiment. Despite some significant discrepancies, the model is capable of representing the general features of ozone and related trace gas profiles over distinct regions. To perform this evaluation, we defined 3 domains for comparing the model results to the aircraft observations: over N.E. US, Europe and the Atlantic corresponding to a pollution remote region, the area affected by this pollution and a region between where the pollution is transported, respectively. In addition, simulated CO and NO_2 are compared to satellite instruments MOPITT and SCIAMACHY data, respectively. We obtain the following results:

1. OH concentrations are relatively well simulated above the boundary layer of N.E. US. The overestimation of about 0.1 pptv observed at lower troposphere over this domain could reflect inaccuracies in our emission inventory. The model systematically overestimates observed OH concentrations by about 0.2-0.4 pptv over the Atlantic domain. This bias may result from both an underestimation of the Atlantic cloud cover by the meteorological ARPEGE analyses and the lack of photochemical effects of aerosols in MOCAGE.

2. The vertical behavior of H_2O_2 over N.E. US is correctly represented by the model. The H_2O_2 overestimation observed over the Atlantic domain is consistent with the OH bias.

3. The model reproduces very well the CO fields. However, there is a slight systematic overestimation of about 10-20 ppbv in the free troposphere which could reflect a

global overestimation of CO emissions. Comparisons with MOPITT CO suggest that the transport processes are particularly well simulated by MOCAGE.

4. The model reproduces quite well the ethane profiles but an underestimation of about 500 pptv is observed within the continental PBL that probably results from too weak emissions in our inventory.

5. Comparisons for HCHO and isoprene show a relatively good agreement between observations and simulation. Comparisons with aircraft measurements and SCIAMACHY NO_2 suggest that we overestimate NO_x anthropogenic emissions over N.E. US and Europe. Above the boundary layer over N.E. US, NO_x concentrations are well simulated except in the upper troposphere where NO_x production by lightning is not yet parameterized in this version of MOCAGE. The underestimation of 100-200 pptv over the Atlantic and Europe domains is probably due to the excess of OH in the model. However, over the Atlantic the discrepancies remain within the range of observations. In the opposite, NO_2 tropospheric columns from SCIAMACHY are overestimated by the model, which could reflect a large impact of the Atlantic cloud cover on the NO_2 retrieval errors. In addition, comparisons with NO_2 from SCIAMACHY pointed out that the daily US emission inventory overestimates the NO_x emissions over wildfire areas. This explains the near systematic bias in PAN concentrations of about 500 pptv in the model. HNO_3 profiles are relatively well reproduced except in the Atlantic marine boundary layer where the model probably underestimates wet scavenging processes.

6. O_3 profiles show an overestimation of about 30 ppbv in the lower troposphere of the N.E. US domain, which could result from recent changes in trace gas precursors emissions over the US. Over the Atlantic, the overestimation is about 10-30 ppbv. The simulated

ozone profile over Europe fits well with the observed profile. We note that globally, the ozone bias are well correlated with the NO_y bias.

Therefore, this study suggests that improvements are needed in our global and daily emission inventory, especially for NO_x species, to better simulate the ozone and related trace gas concentrations. Further work will be done soon using a new version of MOCAGE with a lightning NO_x parameterization and new emission factors.

Acknowledgments.

N. B., J.L.A. and V.H.P. acknowledge financial support from national programmes (PNCA, PATOM) provided by INSU, ADEME, Météo France, CNES as well as the Institut Geographique National (IGN) for hosting the DLR Falcon campaign at Creil, France. We also would like to thank the whole ICARTT team, and in particular, UK BAe-146 scientists (Lisa Whalley and Jim Hopkins for PAN and VOC data) and NASA DC8 scientists (Bill Brune (NO data), Ron Cohen (NO_2 data) Jack Dibb (HNO_3 data), Glen Diskin (water vapor), Vince Brackett and John Hair for aerosol data and aerosol optical depth retrievals). We also express our gratitude to Philippe Nédélec for provision of MOZAIC O_3 and CO data and to the NCAR MOPITT team for providing data. The National Center for Atmospheric Research is sponsored by the National Science Foundation

References

Barthe, C., J.-P. Pinty, and C. Mari (2006), Lightning-produced NO_x in an expicit electrical scheme: a STERAO case study, *J. Geophys. Res.*, submitted.

Bechtold, P., et al. (2001), A mass flux convection scheme for regional and global models, *Quart. J. Roy. Meteor. Soc.*, 127, 869–886.

Bertschi, I., et al. (2003), Trace gas particle emission from fires in large diameter and below ground biomass fuels, *J. Geophys. Res.*, *108*(D13), 8472, doi:10.1029/2002JD002100.

Bey, I., et al. (2001), Global modeling of tropospheric chemistry with assimilated meteorology: Model description and evaluation, *J. Geophys. Res.*, Vol.106, No. D19, 23,073-23,095.

Bovensmann, H. et al. (1999), SCIAMACHY - Mission objectives and measurement modes, *J. Atmos. Sci.*, 56 (2), 127-150.

Brune, W. H., et al. (1998), Airbone in-situ OH and HO_2 observations in the cloud-free troposphere and lower stratosphere during SUCESS, *J. Geophys. Res.*, Vol.25, No.10, pages 1701-1704.

Chandra, S., et al. (2004), Elevated ozone in the troposphere over the Atlantic and Pacific oceans in the Northern Hemisphere, *Geophys. Res. Let*, *31*, L23102, doi:10.1029/2004GL020821.

Courtier, P., et al. (1991), The ARPEGE project at Météo-France, *Workshop on numerical methods in atmopheric models.*, Vol.2, 193-231, ECMWF, Reading, UK.

Decaria, A. J., et al. (2005), Lightning generated NO_x and its impact on tropospheric ozone production: A three-dimensional modeling study of a Stratospheric-Troposphere Experiment: Radiation, Aerosols and Ozone (STERAO-A) thunderstorm, *J. Geophys. Res.*, *110*, D14303, doi:10.1029/2004JD005556.

Deeter, N., et al. (2004), Vertical resolution and information content of CO profiles retrieved by MOPITT, *Geophys. Res. Lett.*, *31*, L15112, doi:10.1029/2004GL020235.

Deeter, N., et al. (2003), Operational carbon monoxide retrieval algorithm and selected result for the MOPITT instrument, *J. Geophys. Res.*, *108*(D14), 4399, doi:10.1029/2003JD0031186.

Dentener, F., D. Stevenson, K. Ellingsen, T. van Noije, M. Schultz en al. (2006), The global atmospheric environment for the next generation, *Environmental Science and Technology*, accepted.

Dentener, F., et al. (2004), The Impact of air pollutant and methane emission controls on tropospheric ozone and radiative forcing : CTM calculations for the period 1990-2030, *Atmos. Chem. Phys*, *4*, 1551-1564.

Drummond, J. R., and G. S. Mand (1996): The Measurements of Pollution in the Troposphere (MOPITT) instrument: Overall performance and calibration requirements. *J. Atmos. Oceanic Technol.*, 13, 314-320

Dufour, A., et al. (2005), Observed and modeled "chemical weather" during ESCOMPTE, *Atmos. Res.*, *74* (1-4), 161-189.

Duncan, B. N., et al. (2003), Indonesian wilfires of 1997: Impact on tropospheric chemistry, *J. Geophys. Res.*, *108*(D15), 4458, doi:10.1029/2002DJ003195.

Fensenfeld, F., ICARTT overview (2006), *J. Geophys. Res. This issue*

Fiore, A. M., et al. (2005), Evaluating the contribution of changes in isoprene emissions to surface ozone trends over eastern United States, *J. Geophys. Res. 110*(D12303), doi:10.1029/2004JD005485.

Grewe, V. (2006), The origin of ozone, *Atmos. Chem. Phys. Discuss.*, *6*, 1495-1511..

Helan, J. ,et al. (2003), Aircraft measurements of nitrogen oxides, ozone, and carbon monoxide during MINOS 2001: distributions and correlation analyses. *Atmos. Chem.*

Phys. Discuss., *3*, 1991-2026.

Horowitz, L. W., et al. (2003), A global simulation of tropospheric ozone and related tracers: Description and evaluation of MOZART, version 2, *J. Geophys. Res.*,*108*(D24), 4784, doi:10.1029/2002JD002853.

Hudman, R. C., et al. (2004), Ozone production in transpacific Asian pollution plumes and implications for ozone air quality in California, *J. Geophys. Res.*, *109*, D23S10, doi:10.1029/2004JD004974.

Jacob, D. J. (2000), Handbook of Weather, Climate and Water, *Mc-Graw Hill*.

Josse, B., Simon P. and V.-H. Peuch (2004), Radon global simulations with the multiscale chemistry transport model MOCAGE, *Tellus*, 56B, 339-356.

Lefèvre, F., et al. (1994), The 1991-1992 stratospheric winter: three-dimensional simulations, *J. Geophys. Res.*, *99*, 8183-8195.

Louis, J.-F (1979), A parametric model for vertical eddy-fluxes in the Atmosphere, *Bound. Lay. Meteor.*, *17*, 187-202.

Martin, R. V., et al. (2003), Global and regional decreases in tropospheric oxidant from photochemical effects of aerosols, *J. Geophys. Res.*, *108*(D3), 4097, doi:10.1029/2002JD002622.

Mathieu, A. (2003), Evaluation of a Numerical Weather forecast Model Using Boundary Layer Cloud-Top Temperature retrieved from AVHRR. *Monthly Weather Review*,Vol. 132,No.4,pp.915-298.

Michou, M., et al. (2005), Measured and modeled dry deposition velocities over the ESCOMPTE area, *Atmos. Res.*, *74* (1-4), 89-116.

Michou, M., and Peuch, V.-H. (2002), Surface exchanges in the MOCAGE multi-scale chemistry and transport model. *J. of Water Science*, *15*, 173-204.

Nédélec, P., et al. (2003), An Improved infrared carbon monoxide analyser for routine measurements aboard commercial aircraft: Technical validation and first scientific results of the MOZAIC III programme, *Atmos. Chem. Phys*, *3*, 1551-1564.

Nho-Kim, E.-Y., et al. (2004), Parameterization of size dependent particle dry deposition velocities for global modeling, *Atmos. Env.*, 38, 13, 1933-1942.

Palmer, P. I., et al. (2001), Air-mass factor formulation for spectroscopic measurements from satellites: Application to formaldehyde retrievals from the Global Ozone Experiment, *J. Geophys. Res.*,*104* 14,539-14,550.

Pfister, G., et al. (2005), Quantifying CO emissions from the 2004 Alaskan wildfires using MOPITT CO data, *Geophys. Res. Let.*, *32*, l11809, doi:10.1029/2005GL022995.

Pradier S., J.L. Attié, M. Chong, J. Escobar, V-H. Peuch, J-F Lamarque, B. Kattatov and D. Edwards (2006) : Evaluation of 2001 springtime CO transport over West Africa using MOPITT CO measurements assimilated in a global chemistry transport model *Tellus* 58B, 3, 163-176

Real, E., et al. (2006), Processes influencing ozone levels in Alaskan forest fire plumes during long range transport over the North Atlantic, *this issue*.

Richter, A., and Burrows, J.P. (2002), Retrieval of tropospheric NO_2 from GOME measurements, *Adv. Space Res.*, Vol 29, No. 11,pp. 1673-1683.

Richter, A., Burrows, J. P., Nüβ, H., Granier and C, Niemeier, U. (2005), Increase in tropospheric nitrogen dioxide over China observed from space, *Nature*, 437, 129-132, doi: 10.1038/nature04092, 2005

Rivière, E. D., et al. (2005), Modelling study of the impact of deep convection on the UTLS air composition -PartII: Ozone budget in the TTL, *Atmos. Chem. Phys. Discuss.*, 5, 9169-9205.

Stockwell, W. R., et al. (1997), A new mechanism for regional atmospheric chemistry modelling, *J. Geophys. Res.*, *102*(D22), Pages 25,847-25,879.

Thouret, V., et al. (1998), Comparisons of ozone measurements from the MOZAIC airborne programme and the ozone sounding network at eight locations., *J. Geophys. Res.*, 103, 25695-25720.

Turquety, S. (2006), Inventory of boreal fire emissions for North America in 2004: the importance of peat burning and pyro-convection injection, *J. Geophys. Res.*, submitted.

Wang, Y. et al. (1998), Global simulation of tropospheric O_3-NO_x-hydrocarbon chemistry. 2. Model evalution and global ozone budget, *J. Geophys. Res.*,*103*(D9), Pages 10,727-10,755.

Xiao, Y. (2005), Global budget of ethane and constraints on North American sources from INTEX-A aircraft data, 2005 Fall AGU Meeting, San Francisco.

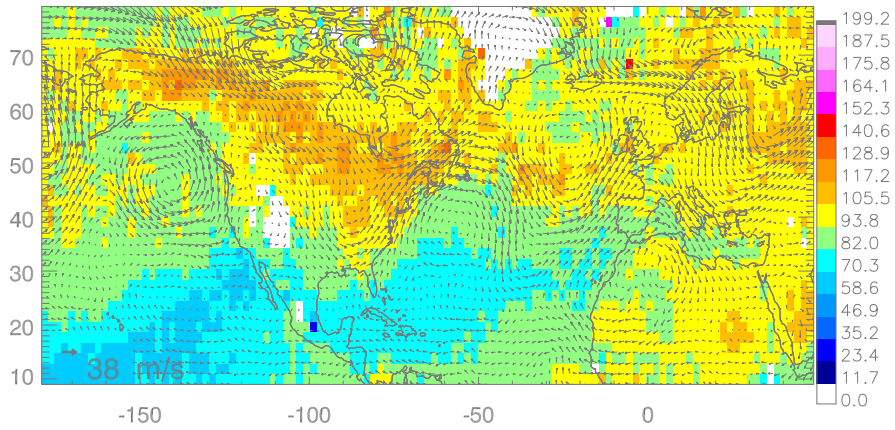

Figure 1. MOPITT CO (ppbv) binned at 2°x 2°and ARPEGE horizontal wind at 500 hPa averaged from July 15 to August 15, 2004.

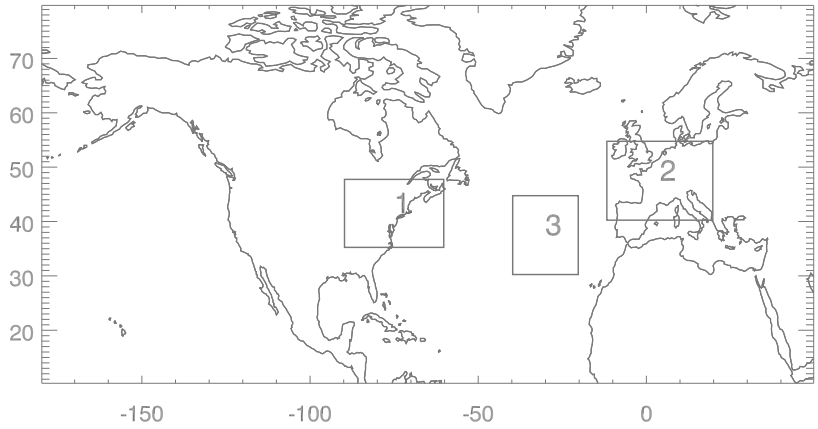

Figure 2. Regions used to aggregate aircraft observations for the purpose of model evaluation. The different boxes represent 1: N.E. US region; 2: Europe region; 3: the Atlantic ocean region.

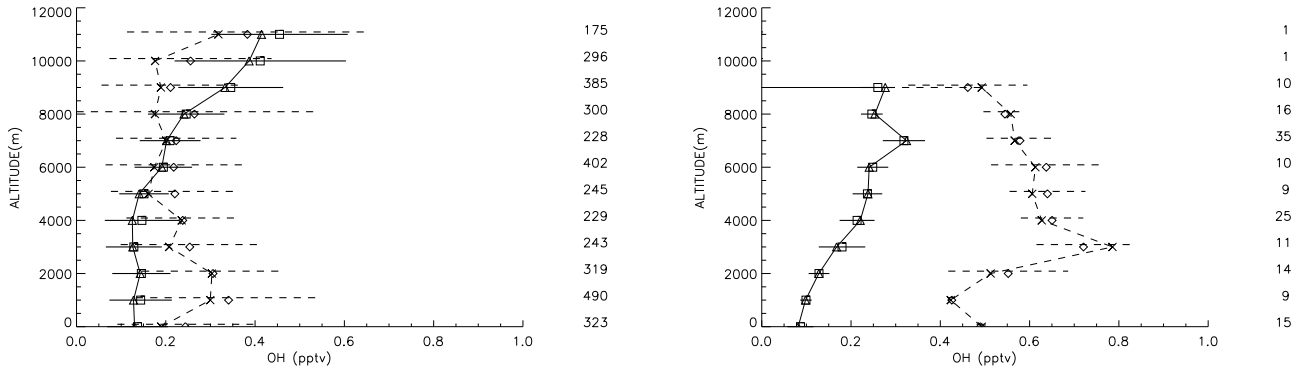

a) **b)**

Figure 3. Comparisons of observed and simulated vertical profiles of OH concentrations (pptv). The open squares are mean observed values (with horizontal bars for standard deviation), and the open triangles and solid lines are median observed values. Open diamond are mean simulated values and cross and dotted lines are median simulated values (with horizontal bars for standard deviations). Values on the right are the number of aircraft data averaged for each level. a): domain 1; b): domain 3.

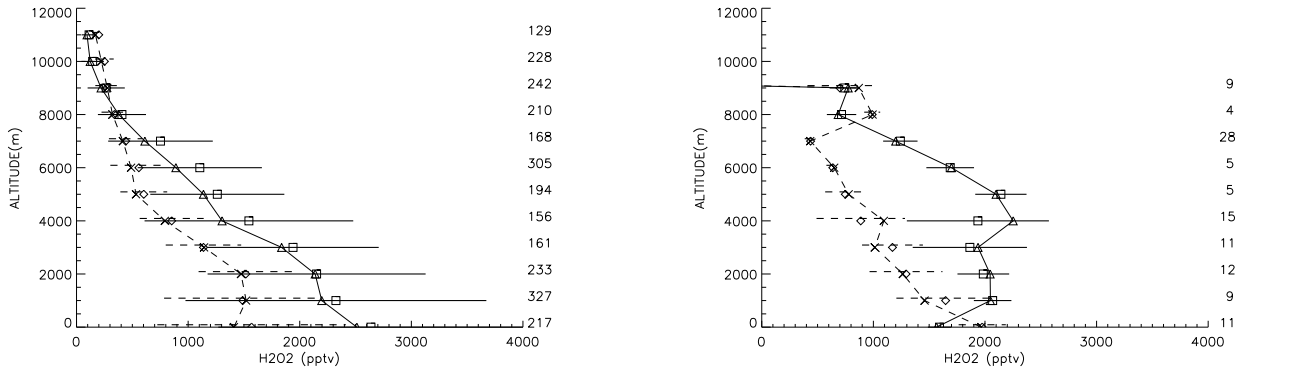

a) **b)**

Figure 4. Same as figure 3 (pptv) but for H_2O_2.

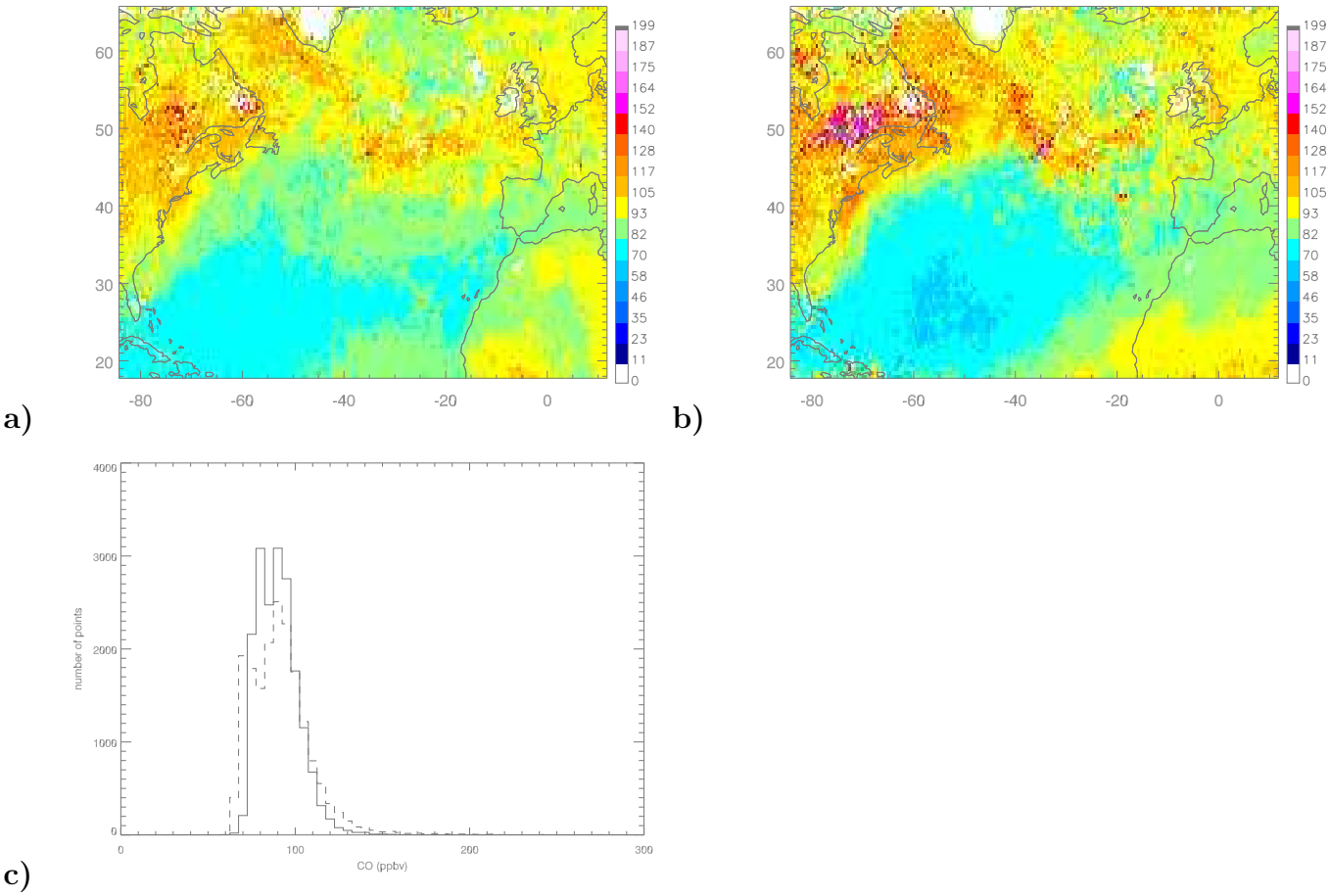

Figure 5. Comparison between MOPITT and MOCAGE CO (ppbv) during ITOP at 500 hPa. a) MOPITT CO binned at 0.5 °x 0.5 °; b) MOCAGE CO; c) corresponding histograms of MOCAGE (dashed line) and MOPITT CO (solid line).

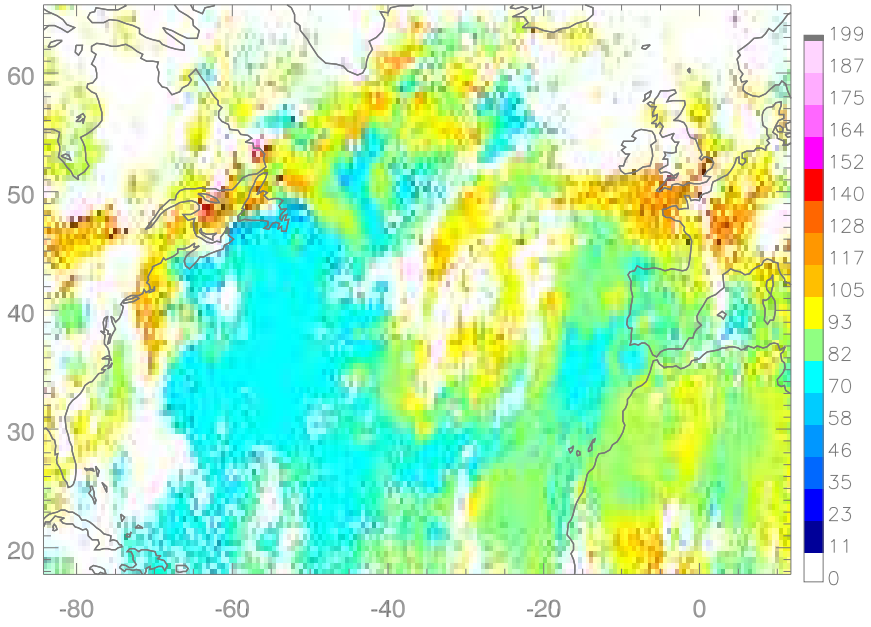

a)

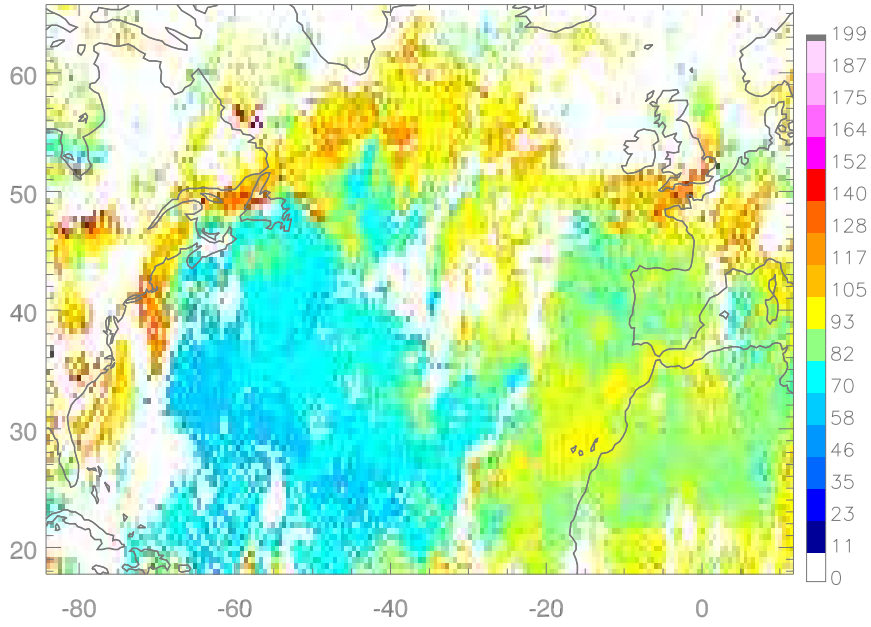

b)

Figure 6. Comparison between MOPITT and MOCAGE CO (ppbv) at 500 hPa for the period between July 24 and July 26, 2004. a) MOPITT CO binned at 0.5 °x 0.5 °; b) MOCAGE CO.

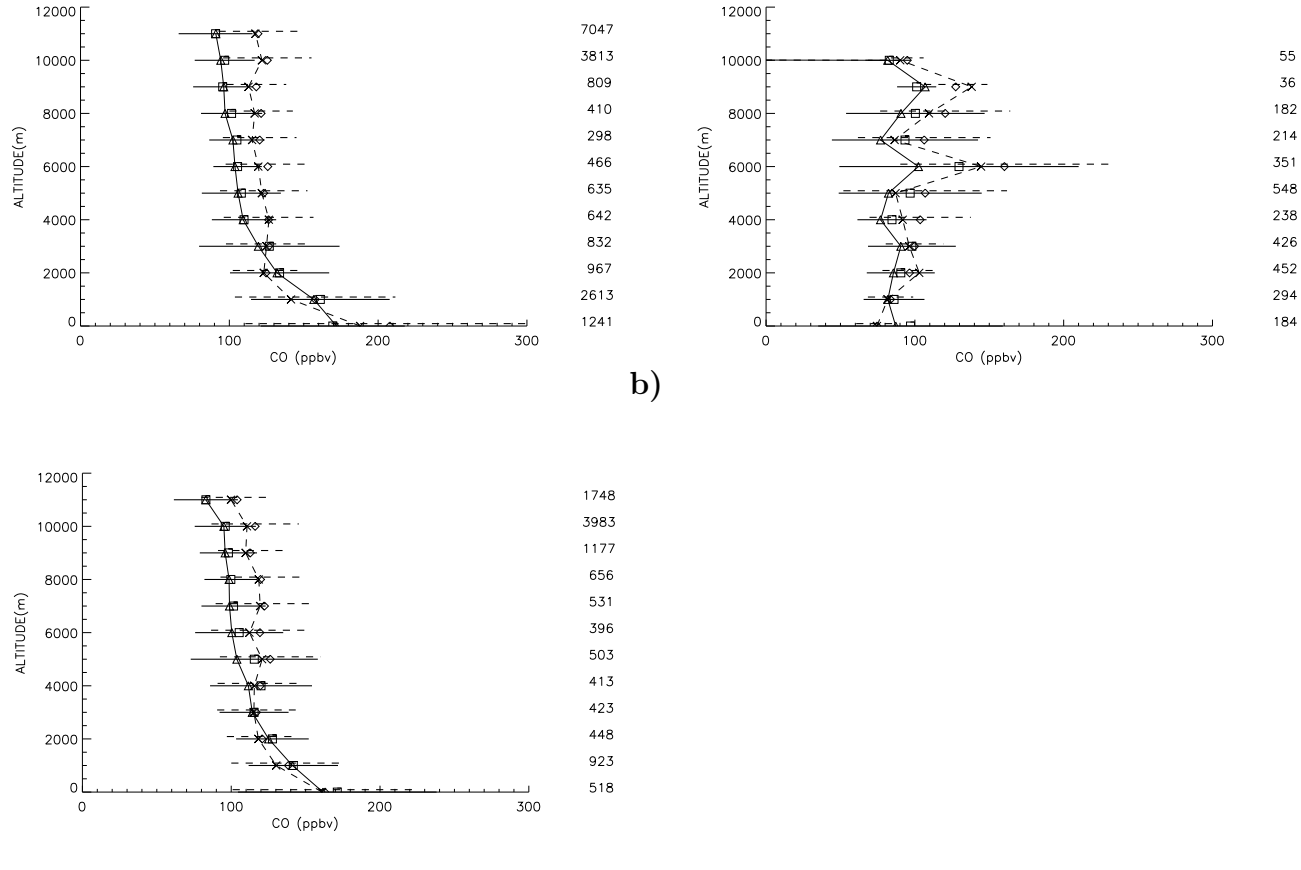

Figure 7. Same as figure 3 but for CO (ppbv) and for a) domain 1; b) domain 3; c) domain 2.

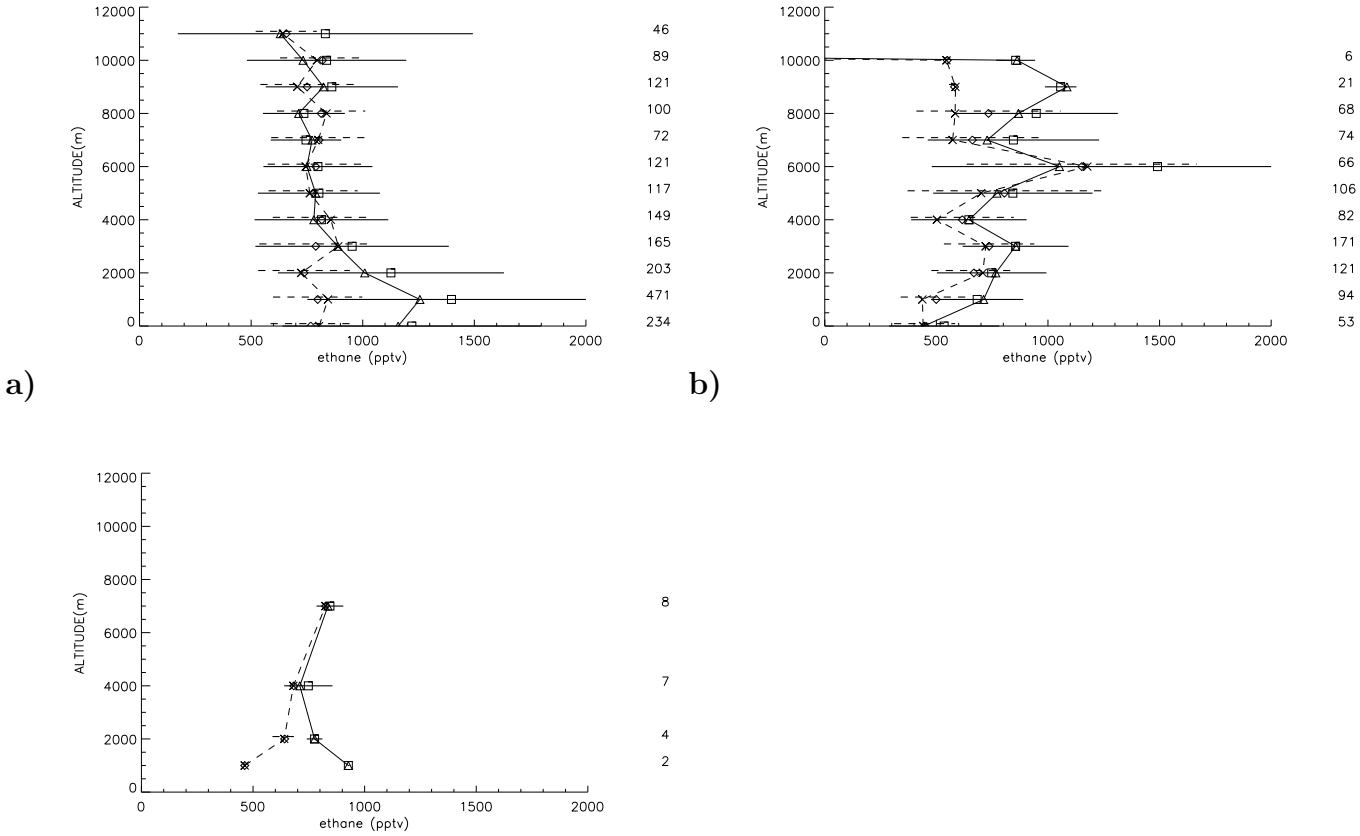

Figure 8. Same as figure 7 but for ethane (pptv).

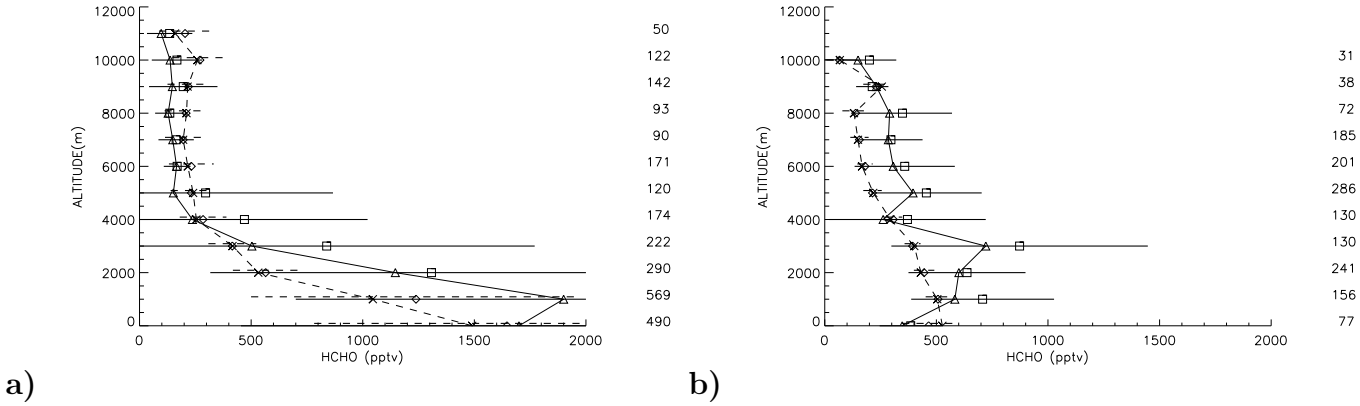

Figure 9. Same as figure 3 but for formaldehyde (HCHO) (pptv).

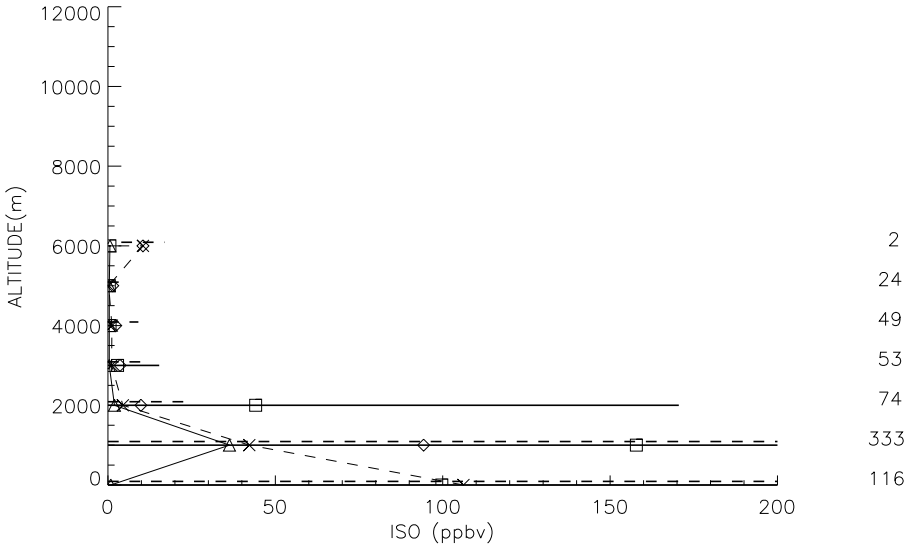

Figure 10. Same as figure 3 but for isoprene (ppbv) and only over domain 1.

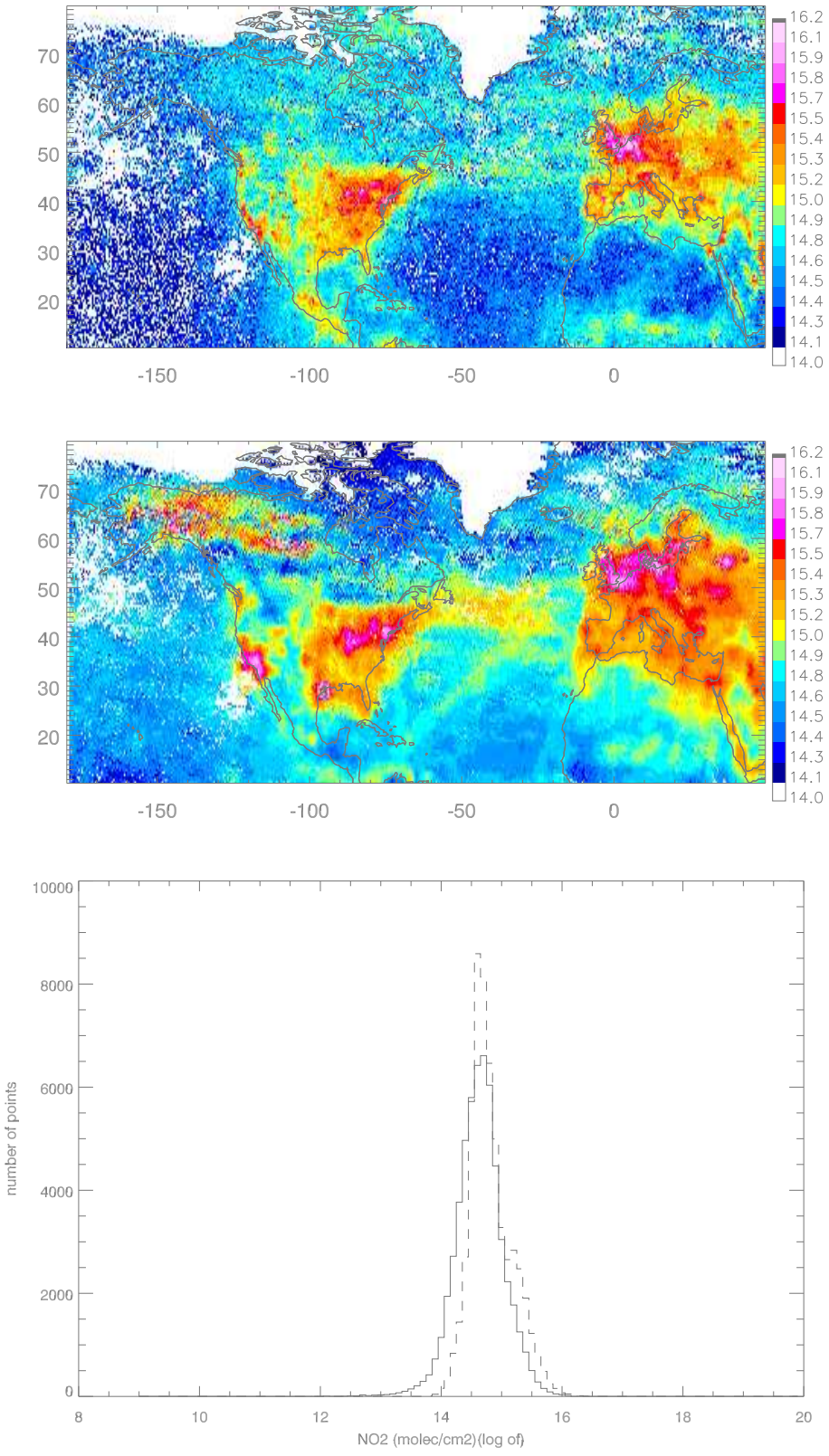

Figure 11. Comparison between SCIAMACHY and MOCAGE NO_2 for the period between July 15 and August 15, 2004. The color code represents the logarithm of NO_2 concentration (molec.cm^{-2}). Top: NO_2 tropospheric columns from SCIAMACHY; Middle: NO_2 tropospheric columns from MOCAGE. Bottom: corresponding histogram of MOCAGE NO_2 (dashed line) and SCIAMACHY NO_2 (solid line).

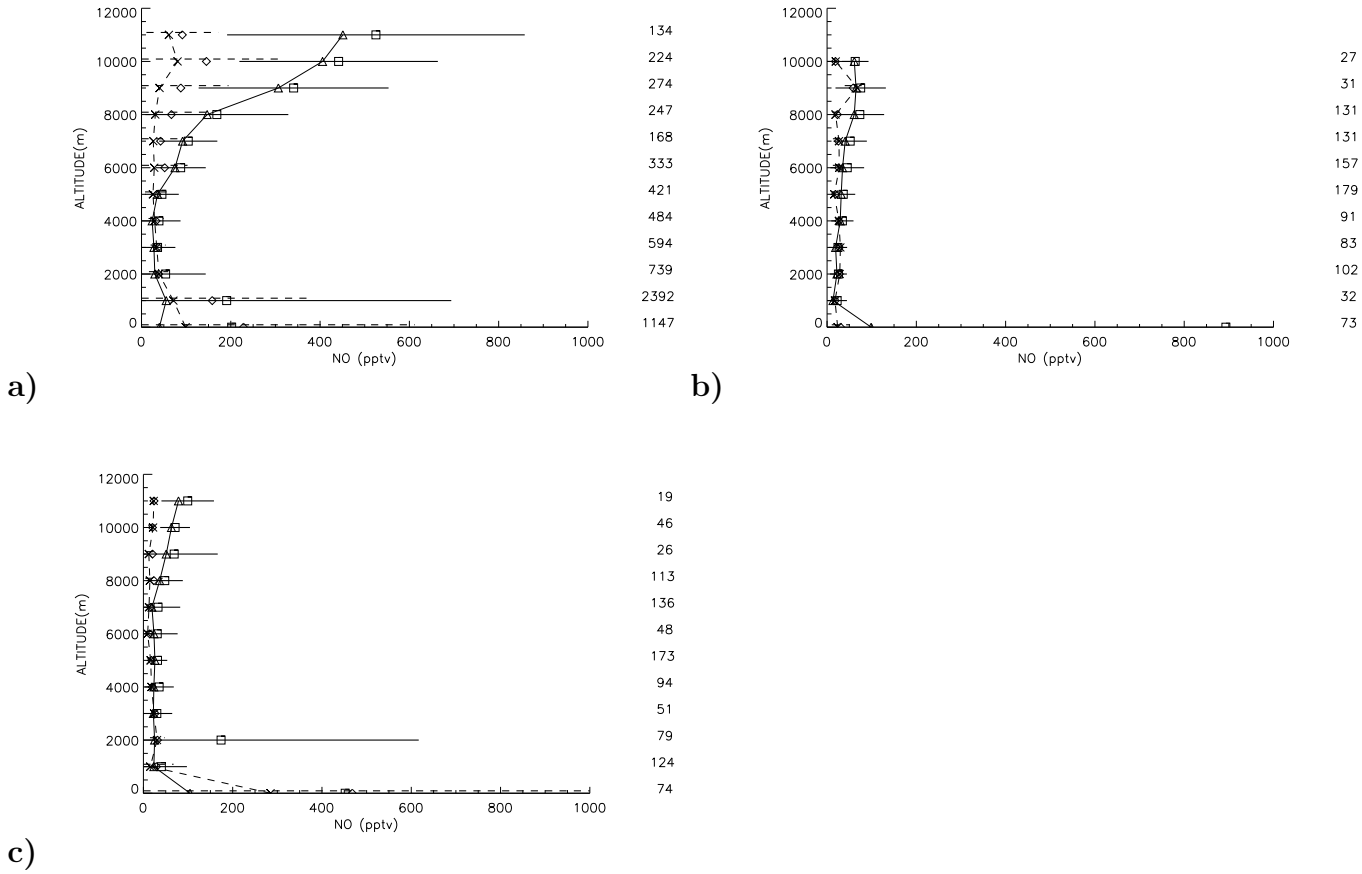

Figure 12. Same as figure 7 but for NO (pptv).

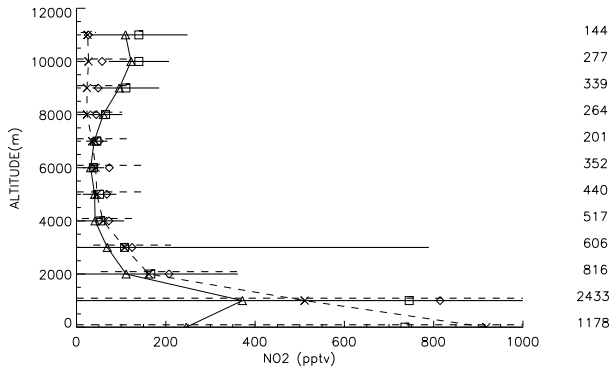

a)

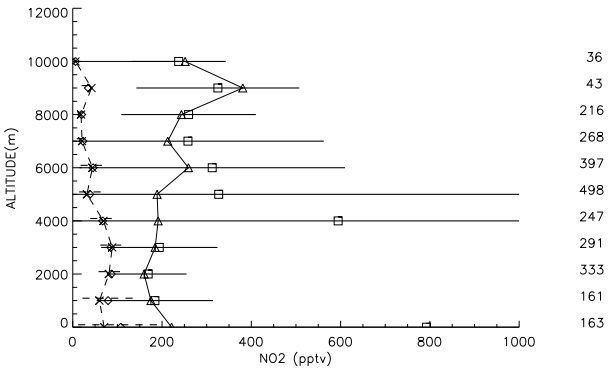

b)

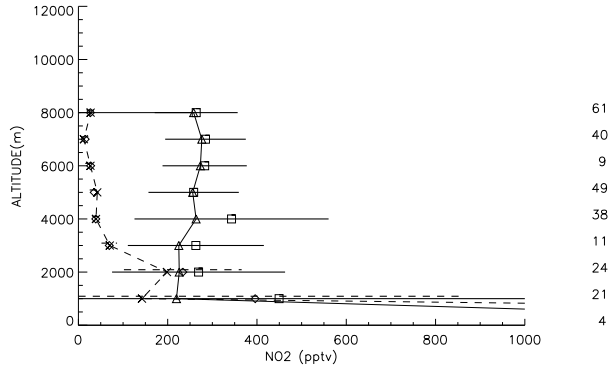

c)

Figure 13. Same as figure 7 but for NO_2 (pptv).

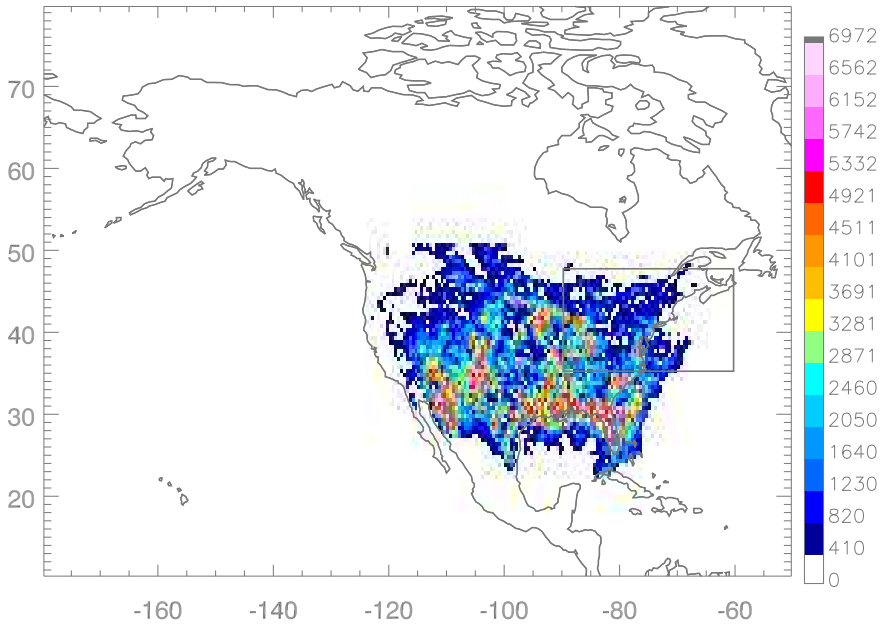

Figure 14. Lightning activity over the US from July 15 to August 15, 2004. The black box delimits the domain 1. Colored pixels indicate the number of cloud-to-ground lightnings averaged over a 0.5 °x 0.5 °grid. (from the National Lightning Detection Network)

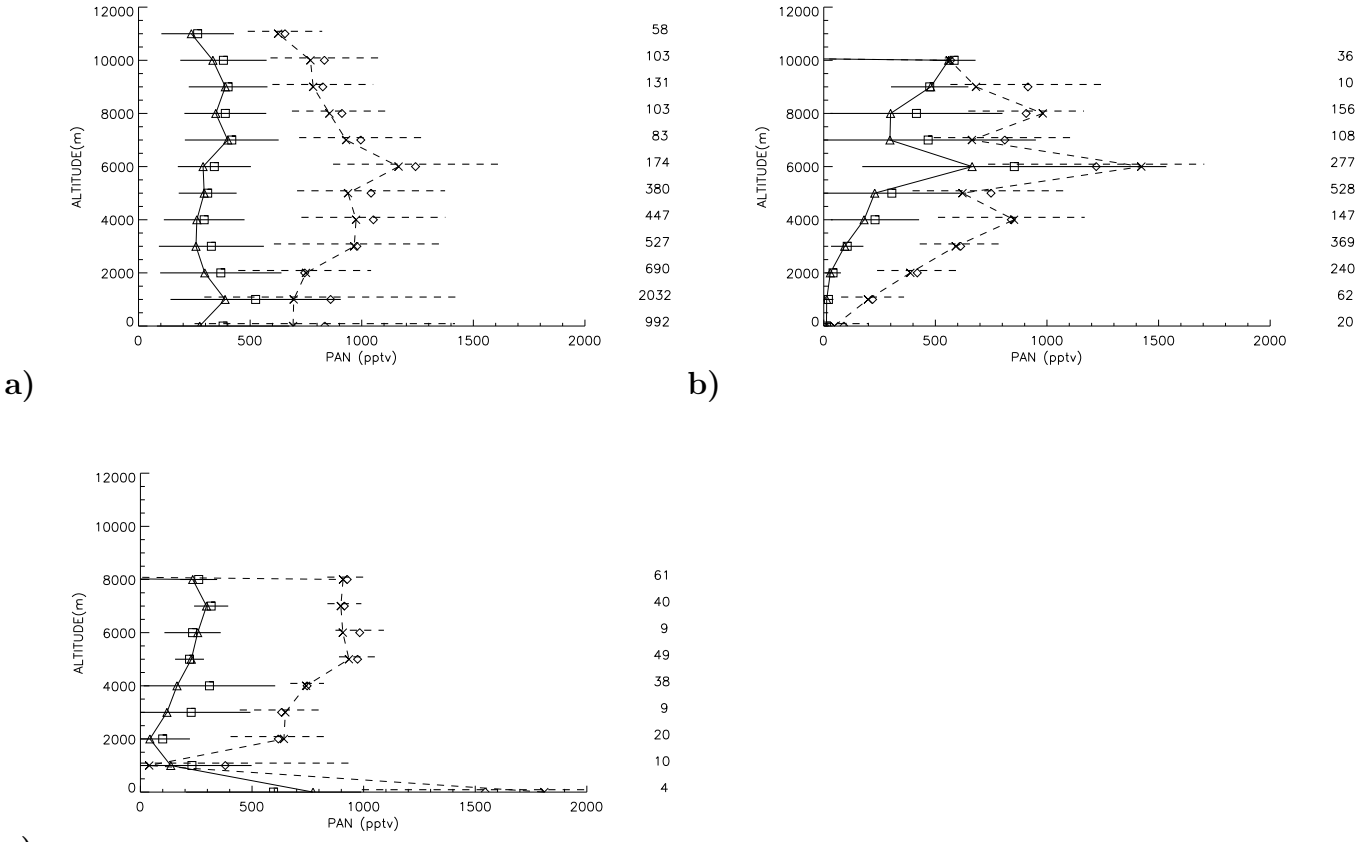

Figure 15. Same as figure 7 but for PAN (pptv).

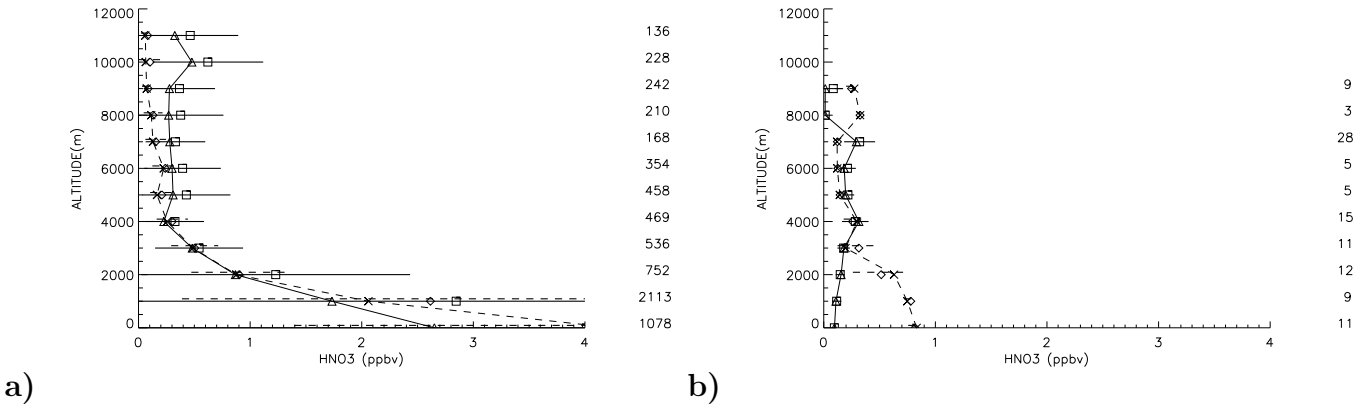

Figure 16. Same as figure 3 but for HNO_3 (pptv).

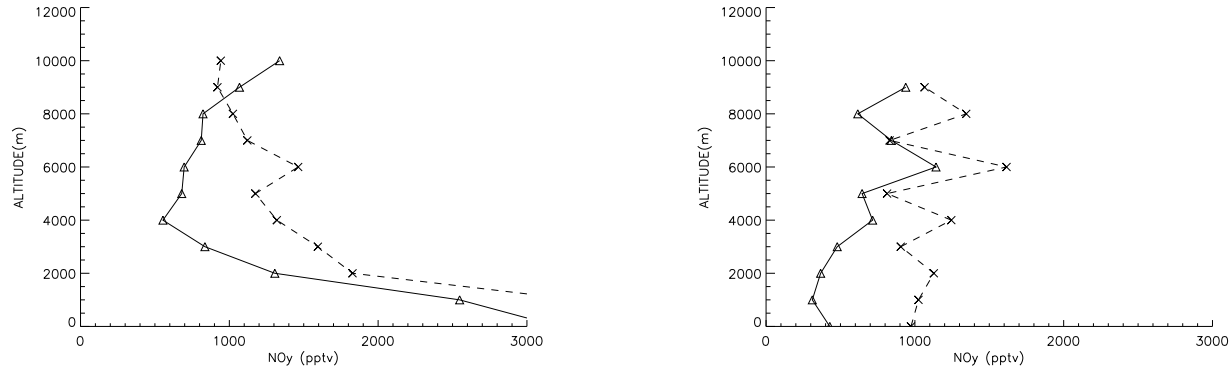

Figure 17. Same as figure 3 but for NO_y (pptv).

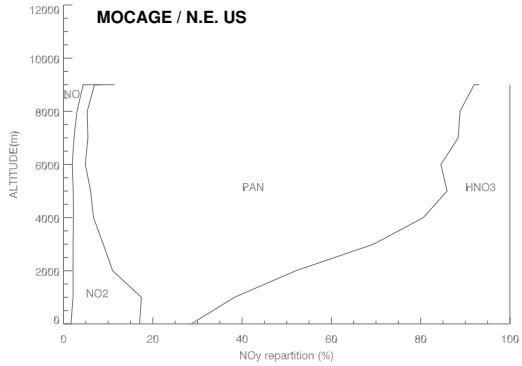

a)

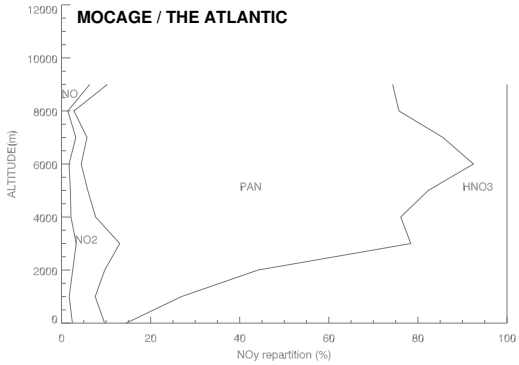

b)

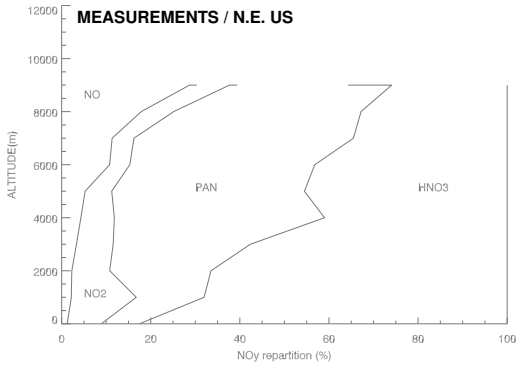

c)

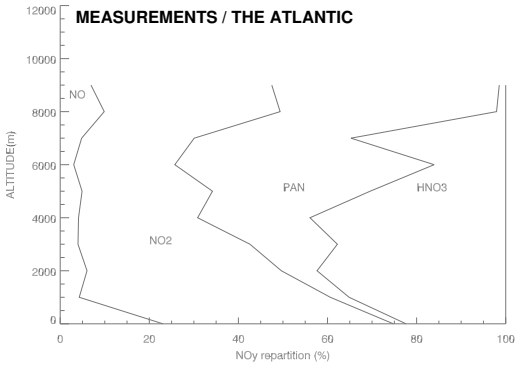

d)

Figure 18. Repartition of the different species for NO_y (%) for the MOCAGE model and the aircraft measurements: a) model over domain 1; b) model over domain 3; c) observations over domain 1; d) observations over domain 3.

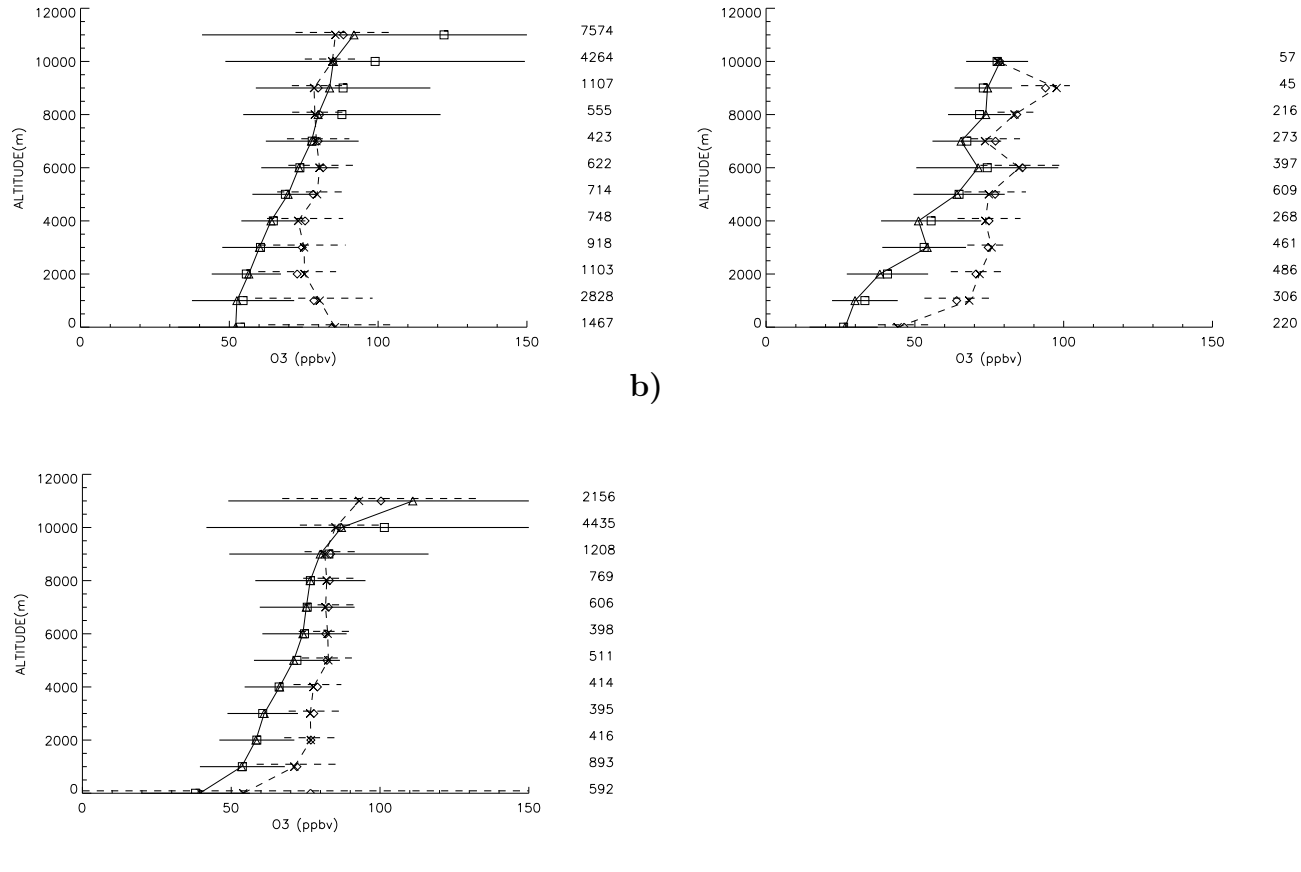

Figure 19. Same as figure 7 but for O_3 (ppbv).

Table 1. MOCAGE emissions inventories used for the ITOP simulation.

[a]Species	Biomass burning	Other sources
CO	(b)	(c)
NO_x	(b)	(c)
TOL	(c)	(b)
CH_4	(b)	(c)
HC_5	(b)	(b)
ALD	(b)	(b)
HCHO	(b)	(b)
HC_3	(b)	(b)
ETH	(b)	(b)
ETE	(b)	(b)
KET	(b)	(b)
OLI	(b)	(b)
OLT	(b)	(b)

[a] see *Stockwell et al.*, [1997] for the acronyms
[b] Daily emissions over the US from *Pfister et al.*, [2005]
[c] from *Dentener et al.* [2004, 2006]

Table 2. Chemical species measured by the different aircraft

BAE-146	P3	DC-8	Falcon	Airbus (MOZAIC)
CO, O_3	CO, O_3	CO, O_3	CO, O_3	CO, O_3
NO, NO_2	NO, NO_2	NO, NO_2	NO	
PAN	PAN, HNO_3	PAN, HNO_3, H_2O_2, OH		
ETH, ISO, HCHO	ETH, ISO, HCHO	ETH, ISO, HCHO		